

# Thermal Ring-Opening Polymerization of Hydrocarbon-Bridged [2]Ferrocenophanes: Synthesis and Properties of Poly(ferrocenylethylene)s and Their Charge-Transfer Polymer Salts with Tetracyanoethylene

James M. Nelson, Paul Nguyen, Ruth Petersen, Heiko Rengel, Peter M. Macdonald, Alan J. Lough, Ian Manners,\* Nandyala P. Raju, John E. Greedan, Stephen Barlow and Dermot O'Hare\*

**Abstract:** The poly(ferrocenylethylene)s  $[\text{Fe}(\eta\text{-C}_5\text{H}_3\text{RCH}_2)_2]_n$  **5a** and **5b** (**a**: R = H, **b**: R = Me) have been prepared by thermal ring-opening polymerization of the corresponding strained hydrocarbon-bridged [2]ferrocenophanes  $[\text{Fe}(\eta\text{-C}_5\text{-H}_3\text{RCH}_2)_2]$  (**4a** and **4b**). An X-ray diffraction study of **4a** indicated significant strain. Polymer **5a** was crystalline and insoluble in common organic solvents and was characterized by solid-state  $^{13}\text{C}$  NMR. Polymer **5b**, which was soluble in organic solvents, was characterized by  $^1\text{H}$  and  $^{13}\text{C}$  NMR, UV/visible spectroscopy and elemental analysis. Its molecular weight distribution was bimodal (gel permeation chromatography:  $M_w = 9.6 \times$

$10^4$ ,  $M_n = 8.6 \times 10^4$  for the high molecular weight fraction,  $M_w = 4.8 \times 10^3$ ,  $M_n = 3.5 \times 10^3$  for the oligomeric fraction), suggesting two polymerization mechanisms. The UV/visible spectrum implied a localized structure for the polymer backbone. Cyclic voltammetry revealed that **5b** undergoes two reversible oxidations in  $\text{CH}_2\text{Cl}_2$  solution at  $-0.25$  and  $-0.16$  V. The redox coupling is indicative of only a small degree of interaction between the iron centres. Ther-

mogravimetric analysis indicated that **5a** and **5b** are thermally stable to ca. 300–350 °C under  $\text{N}_2$ . At higher temperatures they yield ferromagnetic iron carbide ceramics **6a** and **6b** (ca. 50% and 32%, respectively, at 600 °C) together with molecular depolymerization products. The reaction of **5b** with tetracyanoethylene (TCNE) yielded insoluble and soluble oxidized products **11** and **12**, which differed in the degree of oligomerization of the  $\text{TCNE}_x^-$  counterions. These products were characterized by IR, elemental analysis, ESR spectroscopy, and magnetic susceptibility measurements. The last revealed the presence of significant anti-ferromagnetic interactions in **12**.

## Keywords

ceramics · ferrocenes · iron · magnetic properties · polymers

## Introduction

Transition-metal-based molecular and oligomeric materials and their associated charge-transfer salts are of considerable current interest for their redox chemistry and solid-state properties.<sup>[1, 2]</sup> Transition-metal-containing polymers are also attracting growing attention as a consequence of their advantageous processability, their physical and catalytic properties, and their potential use as ceramic precursors.<sup>[3–10]</sup> However, until recently progress in this area has been seriously impeded by the lack of viable synthetic routes to high molecular weight examples of

these materials. With this in mind, we reported the discovery that strained [1]ferrocenophanes with a single silicon atom in the bridge, such as **1**, undergo thermal ring-opening polymerization (ROP) to yield high molecular weight poly(ferrocenylsilane)s **2** (Scheme 1).<sup>[11]</sup> We have subsequently shown that the corresponding germanium-,<sup>[12]</sup> phosphorus-,<sup>[13]</sup> sulfur-,<sup>[14]</sup> and tin-bridged<sup>[15]</sup> [1]ferrocenophanes also polymerize thermally to yield high molecular weight poly(ferrocene)s.<sup>[16]</sup> Recent research has focussed on detailed studies of the synthesis and properties of these interesting materials.<sup>[17–31]</sup>

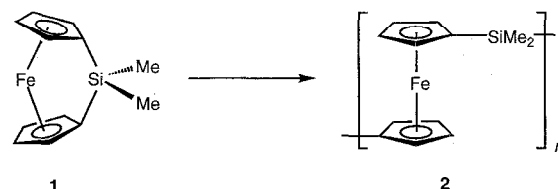
Polymerizable [1]ferrocenophanes possess strained structures in which the planes of the cyclopentadienyl (Cp) ligands are tilted by ca. 14–31° relative to one another.<sup>[13–15, 32–37]</sup> How-

\* I. Manners, J. M. Nelson, P. Nguyen, R. Petersen, H. Rengel, P. M. Macdonald, A. J. Lough

Department of Chemistry, University of Toronto  
80 St. George St., Toronto M5S 3H6, Ontario (Canada)  
Fax: Int. code + (416) 978-6157

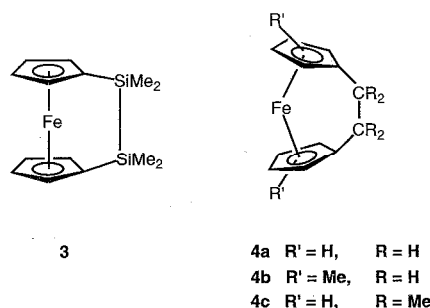
N. P. Raju, J. E. Greedan  
Institute for Materials Research, McMaster University  
Hamilton L8S 4M1, Ontario (Canada)

D. O'Hare, S. Barlow  
Inorganic Chemistry Laboratory, University of Oxford  
South Parks Road, Oxford OX1 3QR (UK)  
Fax: Int. code +(1865) 272 690

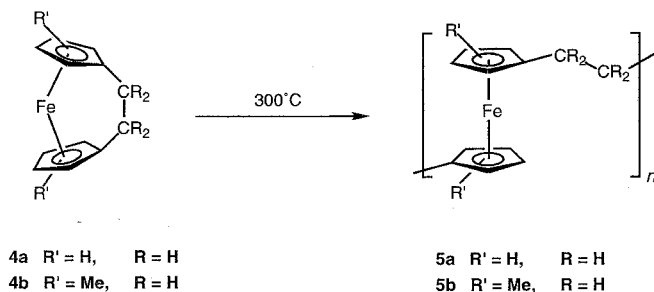


Scheme 1. Thermal ring-opening polymerization of a strained [1]ferrocenophane **1** with a single bridging silicon atom to yield poly(ferrocenylsilane) **2**.

ever, our attempts to extend the ROP methodology to the dilane-bridged [2]ferrocenophane **3** were unsuccessful.<sup>[38]</sup> This was explained by the lower degree of ring strain present in this species, which is reflected by the very small tilt angle of  $4.19(2)^\circ$ .<sup>[38, 39]</sup> As part of our strategy to increase the polymerizability of [2]ferrocenophane systems, we studied the ROP chemistry of [2]ferrocenophanes with a hydrocarbon bridge **4a,b**. These species were prepared by the reaction of the dilithium reagents  $\text{Li}_2[\text{C}_5\text{H}_3\text{RCH}_2]_2$  ( $\text{R} = \text{H}, \text{Me}$ ) with  $\text{FeCl}_2$  in THF. As illustrated by the previously determined structure of **4c**,



which possesses a Cp ring tilt angle of ca.  $23^\circ$ ,<sup>[40]</sup> these species are significantly more strained than **3** because of the smaller size of carbon relative to silicon. We subsequently reported that these hydrocarbon-bridged [2]ferrocenophanes undergo thermally induced ROP to yield poly(ferrocenylethylene)s **5a** and **5b** (Scheme 2).<sup>[41, 42]</sup> We found that the analogous [2]ruthenophanes also polymerize when heated.<sup>[43]</sup>



Scheme 2. Ring-opening polymerization of hydrocarbon-bridged [2]ferrocenophanes to yield poly(ferrocenylethylene)s **5a** and **5b**.

In this paper, we report full details of our work on the ROP of hydrocarbon-bridged [2]ferrocenophanes, and the characterization and properties of the resulting polymers. We also describe studies of the charge-transfer salts derived from the oxidation of poly(ferrocenylethylene)s. Although the electrochemistry of polymers with ferrocene units in their main chain has been the subject of several studies, few recent investigations have been made involving *chemical* oxidation of such polymers. Brandt and Rauchfuss have reported briefly that bromine oxidizes carbon disulfide solutions of high molecular weight poly(ferrocenylene persulfide)  $[\text{Fe}(\eta\text{-C}_5\text{H}_3n\text{Bu})(\eta\text{-C}_5\text{H}_4)\text{S}_2]$  to yield a soluble black material of approximate formula  $[\text{Fe}(\eta\text{-C}_5\text{H}_3n\text{Bu})(\eta\text{-C}_5\text{H}_4)\text{S}_2]_n\text{Br}_{0.5n}$ .<sup>[7a]</sup> Pannell, Diaz and coworkers have used UV/vis spectroscopy to study the oxidation of high molecular weight poly(ferrocenyldialkylsilane)s by iron(III) chlo-

ride.<sup>[26]</sup> We have reported similar studies with  $\text{FeCl}_3$  and, in addition, iodine and *o*-quinone oxidants and have shown that  $\text{I}_2$ -oxidized samples of the high polymer **2** are localized on the  $^{57}\text{Fe}$  Mössbauer timescale at room temperature.<sup>[44]</sup> In a recent, particularly intriguing study by Garnier et al., the oxidation reactions of the low molecular weight oligo(ferrocenyldialkylsilane)s with tetracyanoethylene (TCNE) in dichloromethane were reported to yield dark precipitates; in each case analysis indicated these precipitates contained one TCNE per monomer iron unit, and  $^{57}\text{Fe}$  Mössbauer data showed they contained a mixture of  $\text{Fe}^{\text{II}}$  and  $\text{Fe}^{\text{III}}$  sites, which were localized at 80 K and in rapid exchange at room temperature.<sup>[27]</sup> Although IR data assigned to neutral and ionic polymer units were reported, the  $\text{C}\equiv\text{N}$  stretches of the cyanocarbon counterions were not discussed. The authors interpreted the magnetic data as indicative of both ferromagnetic and spin glass behaviour. This is quite surprising given that one would expect the first oxidation potentials of these materials to be close to those of ferrocene and the fact that ferrocene forms a complex with TCNE, which only dissociates to ionic species in polar solvents. The observation of room-temperature Mössbauer detrapped behaviour in this class of bridged metallocene system is also highly unusual.

We have recently described the oxidation reactions of a number of high molecular weight poly(ferrocenylsilane)s with TCNE,<sup>[45]</sup> which were carried out in analogous fashion to those described by Garnier et al.<sup>[27]</sup> Poly(ferrocenylsilane)s lacking ring methylation gave no reaction with TCNE; this contrasts with the results reported by Garnier et al. for apparently analogous low molecular weight oligomers. However, cyclopentadienyl methylated polymers did react with TCNE, consistent with the effect of methylation upon their oxidation potentials. IR spectroscopy showed unusual cyanocarbon anions to be present. In this paper we also describe the analogous reaction between poly(ferrocenylethylene)s and TCNE.

## Experimental Section

**Materials:** Dicyclopentadiene, methylcyclopentadiene dimer, hexamethylphosphoramide (HMPA) and 1,2-dibromoethane were purchased from Aldrich and were distilled before use. Iron(II) chloride (Aldrich), sodium metal (Aldrich), 1.6 M *n*BuLi in hexanes (Aldrich),  $\text{PtCl}_2$  (Strem) and platinum divinyltetramethylsiloxane complex in xylene (United Chemical Technologies) were used as received. Bis(cyclooctene)rhodium(I) chloride dimer<sup>[46]</sup> and the dilithium salts  $\text{Li}_2[\text{MeC}_5\text{H}_3\text{CH}_2]_2$  and  $\text{Li}_2[\text{C}_5\text{H}_4\text{CH}_2]_2$ <sup>[47]</sup> were prepared by literature methods. TCNE (Aldrich) was purified by vacuum sublimation.

**Equipment:** All reactions and manipulations were carried out under an atmosphere of purified nitrogen either by means of Schlenk techniques or in an inert-atmosphere glovebox (Vacuum Atmospheres), except for the purification of the polymers **5a** and **5b**, which was carried out in air. Solvents were dried by standard methods, distilled, and then stored under nitrogen over activated molecular sieves. The 200 or 400 MHz  $^1\text{H}$  NMR spectra and 50.3 or 100.5 MHz  $^{13}\text{C}$  NMR spectra were recorded on a Varian Gemini 200 or Unity 400. NMR chemical shifts were referenced to residual protonated solvent peaks. Solid-state  $^{13}\text{C}$  NMR spectra were obtained with a Chemagnetics CMX 300 spectrometer equipped with a Chemagnetics magic angle spinning probe doubly tuned to the resonance frequencies of  $^{13}\text{C}$  (75.3 MHz). Samples were spun in a 7.5 mm o.d. zirconium rotor at a spinning rate of 6000 Hz. A single-contact cross-polarization technique was employed with a contact time of 5 ms and proton decoupling during the signal acquisition. The

proton radial frequency field strength was 50 kHz. Spectra were acquired with a sweep width of 50 kHz, a data size of 2 Hz and a recycle delay of 5 s. All chemical shifts were referenced to external TMS. Room-temperature  $^{57}\text{Fe}$  Mössbauer spectra were obtained by means of a Ranger Scientific Inc. VT-1200 instrument with a MS-1200 digital channel analyzer. The  $\gamma$  source was a 6 mCi  $^{57}\text{Co}$  sample supplied by Amersham. The data were collected in a  $-15.8\text{ mm s}^{-1}$  to  $+15.8\text{ mm s}^{-1}$  range and referenced to Fe foil and processed as described previously. Mass spectra were obtained with the use of a VG 70-250S mass spectrometer operating in Electron Impact (EI) mode. Molecular weights were estimated by gel permeation chromatography (GPC) on a Waters Associates liquid chromatograph equipped with a 510 HPLC pump, U6K injector, ultrastaygel columns with a pore size between  $10^3$ – $10^5\text{ \AA}$ , and a Waters 410 differential refractometer. A flow rate of  $1.0\text{ mL min}^{-1}$  was used and samples were dissolved in a solution of 0.1% tetra-*n*-butylammonium bromide in THF. Ten samples of monodisperse polystyrene in the range  $M_w = 10^3$ – $10^6$  were used as standards for calibration purposes. Elemental analyses were performed by Canadian Microanalytical Service, Delta, B. C. (Canada) and Quantitative Technologies, Whitehouse, NJ (USA) or by the Analytical Department of the Inorganic Chemistry Laboratory, Oxford (UK). UV/Visible spectra were recorded on a Hewlett–Packard 8452 A Diode Array Spectrophotometer with a 1 cm quartz cell: the  $\epsilon$  values quoted have the units  $\text{L mol}^{-1}\text{ cm}^{-1}$  and for the polymers are per repeat unit. IR spectra were recorded on a Mattson Instruments Polaris spectrometer.

A Perkin–Elmer DSC-7 differential scanning calorimeter equipped with a TAC7 instrument controller was used to study thermal behaviour. The thermograms were calibrated with the melting transitions of decane and indium and were obtained at a heating rate of  $10\text{ }^\circ\text{C min}^{-1}$  under dinitrogen. A Perkin–Elmer TGA-7 thermal gravimetric analyzer equipped with a TAC7 instrument controller was used to study polymer thermal stability. The thermograms were calibrated with the magnetic transitions of Nicoseal and Perkalloy and were obtained at a heating rate of  $10\text{ }^\circ\text{C min}^{-1}$  under dinitrogen.

Electrochemical experiments were carried out on a PAR model 273 potentiostat with a Pt working electrode, a W secondary electrode, and an Ag wire reference electrode in a Luggin capillary. Polymer solutions were  $5 \times 10^{-3}\text{ M}$  in  $\text{CH}_2\text{Cl}_2$  with  $0.1\text{ M}$   $[\text{Bu}_4\text{N}][\text{PF}_6]$  as supporting electrolyte. Peak currents were found to be proportional to the square root of the scan rate over the range studied ( $25$  to  $1000\text{ mV s}^{-1}$ ); this indicates that charge transfer is similar to a semi-infinite linear diffusion process.

Wide-angle X-ray scattering data were obtained with a Siemens D 5000 diffractometer employing Ni-filtered  $\text{CuK}\alpha$  ( $\lambda = 1.54178\text{ \AA}$ ) radiation. The samples were scanned at step widths of  $0.02^\circ$  with  $1.0\text{ s}$  per step in the Bragg angle range of  $5$ – $90^\circ$ . Samples for the X-ray studies were prepared by spreading the finely ground polymer on grooved glass slides.

High-resolution SEM with EDX and BEI were carried out by Imagetak Analytical Imaging. Errors in the compositional values obtained are considered to be  $\pm 5\%$  for Fe and  $\pm 10\%$  for C. XPS data was collected on a Leybold MAX200 instrument. Values obtained are based on the integration of the peaks Fe (2p, 3/2,  $708.1\text{ eV}$ ) and C (1s,  $284.6\text{ eV}$ ).

All pyrolyses were carried out under an atmosphere of prepurified nitrogen in a  $36''$  3-zone Lindberg Pyrolysis Oven (Model 55035) with a  $1\frac{5}{8}''$  internal diameter and Thermcraft control system Model 3D1-50-115 (UP27) with type K thermocouples and independent temperature control. A program was created that ramped to the desired temperature over a 1 h period. Polymer samples were loaded in quartz boats,  $2 \times \frac{1}{2} \times \frac{1}{2}''$ , and inserted into quartz pyrolysis tubes  $36''$  long with a  $1''$  external diameter, equipped with quartz liners  $32''$  long with a  $1''$  external diameter. Magnetization measurements were performed with a Quantum Design SQUID magnetometer.

ESR measurements were performed in high purity Spectrosil<sup>TM</sup> quartz tubes with an X-band Varian spectrometer; peaks were referenced by means of a microcrystalline sample of 1,1-diphenyl-2-picrylhydrazyl. Solid-state magnetic susceptibilities were measured on samples loaded in gelatin capsules with a Quantum Design MPMS-7 SQUID magnetometer, operated at fields of 0.1 T.

**Synthesis of the [2]ferrocenophane 4a:** A solution of  $\text{Li}_2[\text{C}_5\text{H}_4\text{CH}_2]_2$  (0.35 g, 2.07 mmol) in THF (40 mL) was added dropwise to a suspension of  $\text{FeCl}_2$  (0.26 g, 2.07 mmol) in the same solvent (40 mL) at  $-78\text{ }^\circ\text{C}$ . The reaction mixture was stirred at this temperature for 3 h and was then allowed to warm to room temperature over a 12 h period. Following solvent removal in vacuo,

dark red microcrystalline **4a** was isolated and purified by vacuum sublimation ( $80\text{ }^\circ\text{C}$ , 10 mmHg). Yield 0.285 g (65%); m.p.  $120\text{ }^\circ\text{C}$ ;  $^1\text{H NMR}$  (200 MHz) ( $\text{C}_6\text{D}_6$ ):  $\delta = 4.6$  (t, 4H, Cp), 3.9 (t, 4H, Cp), 2.6 (s, 4H  $\text{CH}_2\text{CH}_2$ );  $^{13}\text{C NMR}$  ( $\text{C}_6\text{D}_6$ ):  $\delta = 91.2$  (*ipso*, Cp), 68.8, 72.9 ( $\alpha$  and  $\beta$ Cp) 34.1 ( $\text{CH}_2\text{CH}_2$ ); UV/Vis (THF):  $\lambda_1 = 474$  ( $\epsilon_1 = 450$ ),  $\lambda_2 = 268$  (sh,  $\epsilon_2 = 2250$ ),  $\lambda_3 = 220\text{ nm}$  ( $\epsilon_3 = 18500\text{ M}^{-1}\text{ cm}^{-1}$ ); MS (EI, 70 eV):  $m/e = 21$  ( $M^+$ , 100%); elemental analysis for  $\text{C}_{12}\text{H}_{12}\text{Fe}$ : calcd. C 67.9, H 5.6%; found C 67.9, H 5.7%.

**Synthesis of the [2]ferrocenophane 4b:** A solution of  $\text{Li}_2[\text{C}_5\text{H}_3(\text{CH}_3)\text{CH}_2]$  (0.50 g, 2.52 mmol) in THF (40 mL) was added dropwise to a suspension of  $\text{FeCl}_2$  (0.32 g, 2.52 mmol) in the same solvent (40 mL) at  $-78\text{ }^\circ\text{C}$ . The reaction mixture was stirred at this temperature for 3 h and was then allowed to warm to room temperature over a 12 h period. Following solvent removal in vacuo, **4b** was isolated as a viscous red oil and purified by vacuum distillation ( $120\text{ }^\circ\text{C}$ , 10 mmHg). Yield 0.45 g (74%). MS (EI, 70 eV):  $m/e = 240$  ( $M^+$ , 100%), 225 ( $M^+ - \text{CH}_3$ , 45%);  $^1\text{H NMR}$  (200 MHz,  $\text{C}_6\text{D}_6$ ):  $\delta = 4.4$ – $4.1$  (br m, 3H, Cp), 3.7–4.1 (br m, 3H, Cp), 2.5–2.7 (s, 4H,  $\text{CH}_2\text{CH}_2$ ), 1.7–2.2 (s, 6H, Me);  $^{13}\text{C NMR}$  (100.5 MHz,  $\text{C}_6\text{D}_6$ ):  $\delta = 85.6$ – $91.5$  (*ipso*, Cp), 67.0– $80.7$  ( $\alpha$ ,  $\beta$ Cp), 32.3– $34.8$  ( $\text{CH}_2\text{CH}_2$ ), 13.9– $15.5$  (Me). Because of the existence of different isomers the NMR spectra of **4b** consisted of numerous ( $\geq 7$ ) peaks in the regions indicated. UV/Vis (THF):  $\lambda_1 = 470$  ( $\epsilon_1 = 456$ ),  $\lambda_2 = 26$  (sh,  $\epsilon_2 = 2350$ ),  $\lambda_3 = 218\text{ nm}$  ( $\epsilon_3 = 18900\text{ M}^{-1}\text{ cm}^{-1}$ ).

**Ring-opening polymerization of 4a and 4b; synthesis of the poly(ferrocenylethylene)s 5a and 5b:** Polymers **5a** and **5b** were prepared similarly and the general synthesis is illustrated by that of **5b**.

A sample of **4b** (1.00 g, 4.2 mmol) was allowed to polymerize in an evacuated sealed Pyrex tube at  $300\text{ }^\circ\text{C}$  for 1 h. The tube contents became molten and rapidly more viscous and, after 1 h, completely immobile. The polymer product was dissolved in THF (40 mL) over 1 h and the resulting solution concentrated to 5 mL. This was then added dropwise to a large excess of methanol to yield **5b** as a mustard-coloured solid. Yield 0.95 g (95%). After multiple precipitations from THF into methanol, the yields of purified **5b** were generally in the range of 80–95%. Polymerization times varied but were usually  $\approx 45\text{ min}$ –1 h. In some cases the polymer product was yellow-brown particularly in cases where heating lasted for  $> 1\text{ h}$ . This is probably a consequence of small amounts of thermal decomposition (see polymer pyrolysis experiments below).

**5a:** Yellow-brown insoluble material, which was obtained in the form of film directly from the polymerization tube. Solid-state  $^{13}\text{C}$  CP-MAS NMR  $\delta = 90.3$  (*ipso*, Cp), 70.1 ( $\alpha$ ,  $\beta$ Cp), and 37.0 ( $\text{CH}_2\text{CH}_2$ ). Polymer **5a** was extracted with hot  $\text{CH}_2\text{Cl}_2$ . Mass spectrometric analysis of the soluble material from the light orange solution identified the cyclic oligomer  $[\text{Fe}(\text{C}_5\text{H}_4\text{CH}_2)]_x$  ( $x = 2$ – $5$ ): MS (EI, 70 eV):  $m/e = 1060$  ( $x = 5$ , 18%), 844 ( $x = 4$ , 15%), 636 ( $x = 3$ , 32%), 424 ( $x = 2$ , 100%), 212 ( $x = 1$ , 90%) Soxhlet extraction of polymer **5a** in THF for 72 h was successful in producing a small amount of soluble material as a mustard-yellow fibrous powder  $^1\text{H NMR}$  (200 MHz,  $\text{C}_6\text{D}_6$ ):  $\delta = 3.6$ – $4.1$  (br, 8H, Cp), 2.3– $2.8$  (br, 4H  $\text{CH}_2\text{CH}_2$ ); GPC for THF-soluble extract: for first fraction,  $M_w = 8.1 \times 10^4$ ,  $M_n = 6.6 \times 10^4$ , polydispersity = 1.2. For second fraction,  $M_w = 4.8 \times 10^3$ ,  $M_n = 3.5 \times 10^3$ , polydispersity = 1.4.

**5b:** Mustard-yellow to yellow-brown fibrous powder  $^1\text{H NMR}$  (200 MHz  $\text{C}_6\text{D}_6$ ):  $\delta = 3.6$ – $4.1$  (br, 6H, Cp), 2.3– $2.8$  (br, 4H,  $\text{CH}_2\text{CH}_2$ ), 1.6– $2.1$  (br 6H, Me);  $^{13}\text{C NMR}$  (100.5 MHz,  $\text{C}_6\text{D}_6$ ):  $\delta = 83.3$ – $88.5$  (*ipso*, Cp), 67.0– $72.5$  ( $\alpha$ ,  $\beta$ Cp), 31.4– $33.4$  ( $\text{CH}_2\text{CH}_2$ ), 13.9– $15.5$  (Me). Because of the existence of different isomers, the  $^{13}\text{C}$  NMR spectra of **5b** consisted of numerous ( $\geq 7$ ) peaks in the regions indicated. The resonances for the different isomers were unresolved in the  $^1\text{H NMR}$  spectrum. GPC: for first fraction,  $M_w = 9.6 \times 10^4$ ,  $M_n = 8.6 \times 10^4$ , polydispersity = 1.1. For second fraction,  $M_w = 4.8 \times 10^3$ ,  $M_n = 3.5 \times 10^3$ , polydispersity = 1.4. UV/Vis (THF):  $\lambda_1 = 44$  ( $\epsilon_1 = 190$ ),  $\lambda_2 = 268$  (sh,  $\epsilon_2 = 3000$ ),  $\lambda_3 = 218\text{ nm}$  ( $\epsilon_3 = 20000\text{ M}^{-1}\text{ cm}^{-1}$ ); elemental analysis for  $\text{C}_{14}\text{H}_{16}\text{Fe}$ : calcd. C 70.0, H 6.7; found C 69.8, H 6.8%.

#### Mechanistic investigations of the ring-opening polymerization of 4b:

*a) Influence of polymerization time on the molecular weight distribution:* Sealed Pyrex tubes containing **4b** ( $\approx 0.2\text{ g}$ ) were heated at  $300\text{ }^\circ\text{C}$  for i) 15 min, ii) 30 min, iii) 45 min, iv) 1 h, v) 1.5 h and vi) 2.5 h, at which time the contents of each tube were examined by GPC in THF. i) The tube contents were free-flowing and GPC analysis showed no signs of a substantial molecular weight fraction ( $M_w > 1000$ ). ii) After 30 min the tube contents

were viscous and mobile and GPC analysis showed that the polymer present possessed an approximate weight-average molecular weight ( $M_w$ ) of  $8.0 \times 10^4$  and a number-average molecular weight ( $M_n$ ) of  $6.6 \times 10^4$  with no substantial lower molecular weight oligomeric fraction. iii) After 45 min the tube contents were immobile and GPC analysis showed a broad bimodal molecular weight distribution: for the high polymer fraction,  $M_w = 8.1 \times 10^4$ ,  $M_n = 6.3 \times 10^4$ , polydispersity = 1.3, and for the oligomeric fraction,  $M_w = 4.8 \times 10^3$ ,  $M_n = 3.5 \times 10^3$ , polydispersity = 1.4. iv) After 1 h the tube contents were immobile and GPC analysis showed a broad bimodal molecular weight distribution. GPC for the polymeric fraction,  $M_w = 7.8 \times 10^4$ ,  $M_n = 6.2 \times 10^4$ , polydispersity = 1.3; for the oligomeric fraction:  $M_w = 3.8 \times 10^3$ ,  $M_n = 2.7 \times 10^3$ , polydispersity = 1.4. v) After 1.5 h the tube contents were immobile and slightly darkened in colour and GPC analysis showed a broad bimodal molecular weight distribution. GPC for the polymeric fraction:  $M_w = 7.8 \times 10^4$ ,  $M_n = 6.2 \times 10^4$ , polydispersity = 1.3; for the oligomeric fraction:  $M_w = 5.5 \times 10^3$ ,  $M_n = 3.5 \times 10^3$ , polydispersity = 1.6. vi) After 2.5 h the tube contents were immobile and contained a small insoluble fraction (ca. 5%). GPC analysis of the soluble portion showed a broad bimodal molecular weight distribution. GPC for the polymeric fraction,  $M_w = 2.1 \times 10^4$ ,  $M_n = 1.6 \times 10^4$ , polydispersity = 1.3; for the oligomeric fraction,  $M_w = 1.7 \times 10^3$ ,  $M_n = 1.2 \times 10^3$ , polydispersity = 1.4.

b) *Influence of heating on the molecular weight distribution*: In order to determine whether the lower molecular weight fraction is produced as a result of thermal decomposition of the polymer, a tube containing a purified 0.1 g sample of polymer **5b** was heated for 1 h at 300 °C. Analysis of the tube contents after this time by GPC showed no significant change in the molecular weight or in the molecular weight distribution.

**Attempted transition-metal-catalyzed ROP of 4a**: To a solution of **4a** (20 mg, 0.09 mmol) was added bis(cyclooctene)rhodium(I) chloride dimer ( $\approx 2$  mg) in  $C_6D_6$ . This mixture was stirred under nitrogen for 48 h with constant monitoring of the reaction by  $^1H$ NMR spectroscopy. Analysis of this mixture after 48 h showed that no reaction had occurred and no signs of insoluble **5a** were apparent. A  $^1H$ NMR spectrum of the mixture displayed characteristic resonances for the starting compound **4a**.  $^1H$ NMR (200 MHz) ( $C_6D_6$ ):  $\delta = 4.6$  (t, 4H, Cp), 3.9 (t, 4H, Cp), 2.6 (s, 4H,  $CH_2CH_2$ ). Analysis of the reaction mixture by GPC showed no material of substantial molecular weight ( $M_w > 1000$ ). Similar results were obtained with  $PtCl_2$  and Pt divinyltetramethyldisiloxane catalysts.

#### Pyrolysis of the poly(ferrocenylethylene)s **5a** and **5b** under dinitrogen:

a) *TGA studies*: A sample of **5a** (0.02 g) was lightly packed into a TGA pan, which was then inserted in the TGA instrument under a steady flow of nitrogen for approximately one minute. The system was then heated from 25 to 600 °C at a heating rate of 10 °C min<sup>-1</sup>. When the program was complete and the furnace was allowed to cool to room temperature a black, lustrous ceramic product **6a** was formed, yield 0.01 g (50%). This material was found to be readily attracted to a bar magnet. Similar studies with **5b** gave a ceramic yield of 32%.

b) *Pyrolysis of 5b in a tube furnace*: A sample of **5b** (0.50 g) was lightly packed into a quartz boat, which was then inserted into a pyrolysis tube. The tube was purged with a steady flow of nitrogen for approximately one minute. The system was then heated from 25 to 600 °C over 1 h and was then maintained at a constant temperature of 600 °C for a further 4 h. During pyrolysis an orange-red liquid condensed on the cooler parts of the pyrolysis tube downstream from the quartz boat. When the program was complete and the furnace allowed to cool to room temperature, a black, lustrous ceramic product **6b** was formed, yield 0.16 g ( $\approx 30\%$ ). This material was also found to be readily attracted to a bar magnet. For ceramic **6b** (derived from **5b** at 600 °C): for surface, XPS: Fe 1, C 87, Si 1, O 11%. For bulk, EDX: Fe 72, C 24, O 4%. Localized electron-rich sites, EDX: Fe 70, C 5, O 25%. Mössbauer spectroscopy: sextuplet IS = 0.03, MHS = 1.81 mm s<sup>-1</sup>. Magnetization measurements:  $H_c = 257$  G,  $M_r = 0.071 \mu_B/Fe$ ,  $M_s = 0.17 \mu_B/Fe$ . XRD: sharp peaks at  $d$  spacing of 2.025, 1.429, and 1.167 Å assigned to  $\alpha$ -Fe. Other peaks together with several broadened peaks of low intensity (3.396, 2.956, 2.519, 2.467, 2.138, 2.100, 1.973, 1.850, 1.613, 1.482 Å).

The red-orange sublimate was collected by rinsing the pyrolysis tube with hexanes and was also analyzed. Mass spectrometry of the red-orange solution showed that it contained an inseparable mixture, which has been tentatively assigned to the linear methylated compounds  $[Fe(\eta-C_5H_3Me_2)(\eta-C_5H_3-Me)(CH_2)_x]$  (MS (EI, 70 eV):  $m/e = 482$  ( $M^+$ ,  $x = 2$ , 40%), 241 ( $x = 1$ ,

100%)) and the cyclic trimer  $[Fe(\eta-C_5H_3(Me)CH_2)_2]_3$  (MS (EI, 70 eV):  $m/e = 720$  ( $M^+$ , 5%)).

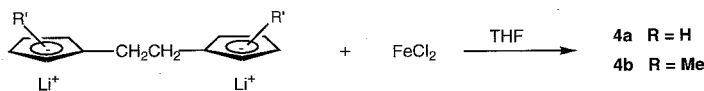
**Reaction of the poly(ferrocenylethylene) **5b** with TCNE**: Experiments were performed on samples of **5b** that had been purified anaerobically. A solution of TCNE (138 mg, 1.08 mmol) in 10 mL  $CH_2Cl_2$  was added to a solution of purified polymer **5b** (250 mg, 1.04 mmol) in 15 mL  $CH_2Cl_2$ . The solution instantly darkened and a dark precipitate slowly appeared. After 12 h the solid was filtered off, washed with 50 mL  $CH_2Cl_2$  and dried in vacuo to yield a black powder, **11** (60 mg). Analysis (%): found (calcd. for the idealized composition  $[Fe(C_5H_3MeCH_2)_2]_n[TCNE]_n$ ) C 66.41 (65.24), H 4.24 (4.38), N 13.20 (15.22), Fe 13.58 (15.17); ESR (solid 6.6 K): cation  $g_{\perp} = 1.70$ ,  $g_{\parallel} = 3.76$ ,  $\langle g \rangle = 2.58$ ; anion  $g = 2.00$ . Selected IR data (nujol mull): 2153 (br), 2198 (br) cm<sup>-1</sup>. The soluble portion was concentrated to 15 mL and added dropwise to vigorously stirred diethyl ether (175 mL). The precipitate was collected by filtration, washed with diethyl ether (100 mL) and dried in vacuo to yield a green powder (95 mg), **12**. Analysis (%): found (calcd. for the idealized composition  $[Fe(C_5H_3MeCH_2)_2]_n[TCNE]_n$ ) C 71.11 (65.24), H 4.86 (4.38), N 13.00 (15.22), Fe 12.55 (15.17); SQUID:  $\mu_{eff} = 1.7 \mu_B$ ,  $\theta = -11.6$  K; ESR ( $CH_2Cl_2$  glass, 6.8 K): cation  $g_{\perp} = 1.70$ ,  $g_{\parallel} = 3.81$ ,  $\langle g \rangle = 2.60$ ; anion  $g = 2.00$ ; selected IR data (nujol mull): 2148 (br), 2199 (br), 2218 (br) cm<sup>-1</sup>.

## Results and Discussion

Ferrocenyl groups have been introduced into the side-group structure of a wide range of organic macromolecules.<sup>[48]</sup> Poly(ferrocenylmethylene)s, of reported structure  $[Fe(\eta-C_5H_4)_2-CH_2]_n$ , have been previously prepared by the zinc chloride/hydrogen chloride-catalyzed polymerization of ((dimethylamino)methyl)ferrocene reported by Neuse and Quo.<sup>[49]</sup> These materials are generally of low molecular weight (< 10000) and have been found to exist as a mixture of 1,2-, 1,3-, and 1,1'-disubstituted ferrocene units in the main chain.<sup>[48]</sup> To our knowledge, no well-characterized poly(ferrocenylethylene)s of substantial molecular weight have been reported although oligomers as well as cyclics are formed in the synthesis of **4a**.<sup>[50, 51]</sup> In our initial communication,<sup>[41]</sup> we reported the thermal ROP of hydrocarbon-bridged [2]ferrocenophanes as a route to high molecular weight poly(ferrocenylethylene)s. In this paper, we discuss in detail the synthesis and properties of the resulting poly(ferrocenylethylene)s and the characteristics of their charge-transfer salts with TCNE.

**Synthesis and characterization of the hydrocarbon-bridged [2]ferrocenophanes **4a** and **4b****: Ferrocenophanes containing hydrocarbon bridges have been known since the initial report of the methylated ethylene-bridged monomer **4c** by Burke Laing and Trueblood,<sup>[40]</sup> which was prepared by the coupling of 6,6-dimethylfulvene with Na in THF to give the bis(cyclopentadienyl)tetramethylethane dianion, followed by the addition of  $FeCl_2$ . The hydrocarbon-bridged [2]ferrocenophane **4c** possesses a substantially ring-tilted structure, as indicated by single-crystal X-ray diffraction studies, which showed that the cyclopentadienyl ligands are significantly tilted by  $\approx 23^\circ$  with respect to one another.

In the work described in this paper, compounds **4a** and **4b** (which consists of a mixture of isomers) were prepared by reaction of the dilithium reagent  $Li_2[(C_5H_3RCH_2)_2]$  with iron(II) chloride in THF solutions (Scheme 3). Lentzner and Watts<sup>[52]</sup> initially reported this synthesis of **4a**; however, these re-

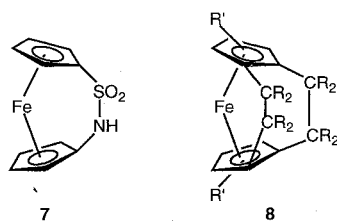


Scheme 3. Preparation of compounds **4a** and **4b** by reaction of  $\text{Li}_2[(\text{C}_5\text{H}_3\text{RCH}_2)_2]$  with iron(II) chloride in THF.

searchers experienced difficulty achieving high yields (yield = 3%) of the starting dilithium compound, owing to the formation of the spirocyclic by-product, spiro[2,4]hepta-4,6-diene. The dilithium reagents used here were prepared by the improved method reported by Collins and coworkers,<sup>[4,7]</sup> which involves the addition of hexamethylphosphoramide (HMPA) to the NaCp/1,2-dibromoethane mixture. The [2]ferrocenophanes were isolated as red, moisture-sensitive materials in  $\approx 70\%$  yield by vacuum sublimation or distillation. The structures of the [2]ferrocenophanes **4a** and **4b** were confirmed by  $^1\text{H}$  and  $^{13}\text{C}$  NMR spectroscopy and by mass spectrometry. This afforded data similar to that reported for the previously prepared methylated [2]ferrocenophane compound **4c**. In the case of **4a**, the molecular structure was also determined by single-crystal X-ray diffraction (see below). The UV/visible spectra of **4a** and **4b** in the 200–800 nm range contained low-energy bands in the visible region at 470–474 nm ( $\epsilon = 450\text{ M}^{-1}\text{ cm}^{-1}$ ) that showed a characteristic bathochromic shift and increase in intensity relative to the long-wavelength band of ferrocene at 440 nm ( $\epsilon = 90\text{ M}^{-1}\text{ cm}^{-1}$ ). Osborne and co-workers have previously commented that this is indicative of significant tilting of the cyclopentadienyl rings.<sup>[53]</sup> Similar bathochromic shifts were also detected for the methylated [2]ferrocenophane **4c** ( $\lambda = 472\text{ nm}$ ,  $\epsilon = 400\text{ M}^{-1}\text{ cm}^{-1}$ ), which was found to possess a significantly ring-tilted structure with a tilt angle of  $23(1)^\circ$ .<sup>[52]</sup>

**Discussion of the X-ray structure of 4a:** Several [2]ferrocenophanes have been crystallographically characterized, including the previously mentioned methylated [2]ferrocenophane **4c**<sup>[40]</sup> and the unstrained disilane **3**,<sup>[38,39]</sup> as well as the S–N bridged [2]thiazaferrocenophane **7** reported by Abramovitch and co-workers,<sup>[54]</sup> which was found to possess a substantially strained, ring-

tilted structure (tilt angle of  $23^\circ$ ). Very recently, Hafner and coworkers<sup>[55]</sup> published the synthesis and X-ray structural analysis of a doubly strapped hydrocarbon-bridged [2]ferrocenophane **8** ( $\text{R} = \text{R}' = \text{H}$ ), which was found to possess a considerably ring-tilted structure with a tilt angle of  $28.8^\circ$ . In order to study further the influence of a hydrocarbon bridge on the strain and polymerizability of these ferrocenophane systems, an X-ray crystallographic study of **4a** was carried out. Crystals of **4a** were isolated from hexanes solution at  $-20^\circ\text{C}$ . The molecular structure of **4a** is shown in Figure 1. A summary of cell constants and data collection parameters are included in Table 1, and important bond lengths and angles are listed in Table 2. The angles  $\alpha$ ,  $\beta$  and  $\delta$  used in discussing the structures are defined in Figure 2. The structure of **4a** is disordered over two sites (C(12a), C(12b)) with occupancies of 0.60 and 0.40.



tilted structure (tilt angle of  $23^\circ$ ). Very recently, Hafner and coworkers<sup>[55]</sup> published the synthesis and X-ray structural analysis of a doubly strapped hydrocarbon-bridged [2]ferrocenophane **8** ( $\text{R} = \text{R}' = \text{H}$ ), which was found to possess a considerably ring-tilted structure with a tilt angle of  $28.8^\circ$ . In order to study further the influence of a hydrocarbon bridge on the strain and polymerizability of these ferrocenophane systems, an X-ray crystallographic study of **4a** was carried out. Crystals of **4a** were isolated from hexanes solution at  $-20^\circ\text{C}$ . The molecular structure of **4a** is shown in Figure 1. A summary of cell constants and data collection parameters are included in Table 1, and important bond lengths and angles are listed in Table 2. The angles  $\alpha$ ,  $\beta$  and  $\delta$  used in discussing the structures are defined in Figure 2. The structure of **4a** is disordered over two sites (C(12a), C(12b)) with occupancies of 0.60 and 0.40.

Table 1. Summary of crystal data and intensity collection parameters for **4a** [a].

empirical formula	$\text{C}_{12}\text{H}_{12}\text{Fe}$
$M_r$	212.07
crystal size (mm)	$0.31 \times 0.28 \times 0.26$
crystal class	orthorhombic
space group	$Pbca$
$T$ (K)	294
$a$ ( $\text{\AA}$ )	7.421(1)
$b$ ( $\text{\AA}$ )	12.305(2)
$c$ ( $\text{\AA}$ )	19.839(4)
$V$ ( $\text{\AA}^3$ )	1811.6(5)
$Z$	8
$\rho_{\text{calc}}$ ( $\text{g cm}^{-3}$ )	1.555
$\mu$ ( $\text{Mol wt}^{-1}$ ) ( $\text{cm}^{-1}$ )	16.05
$F(000)$	880
$\omega$ scan width ( $^\circ$ )	$0.80 + 0.35 \tan \theta$
range $\theta$ collected	$2.05\text{--}24.96$
indep. reflns	1584
no. observed [ $I > 2\sigma(I)$ ]	1118
$R_1$ [ $I > 2\sigma(I)$ ] [b]	0.0520
$wR_2$ [c]	0.1542
GoF	1.123
parameters refined	119
max. density in $\Delta F$ map ( $\text{e}\text{\AA}^{-3}$ )	0.681

[a] Crystallographic data (excluding structure factors) for the structure reported in this paper have been deposited with the Cambridge Crystallographic Data Centre as supplementary publication no. CCDC-100124. Copies of the data can be obtained free of charge on application to The Director, CCDC, 12 Union Road, Cambridge CB21EZ, UK (Fax: Int. code + (1223) 336-033; e-mail: deposit@chemcrs.cam.ac.uk). [b]  $R_1 = \sum(F_o - F_c)/\sum(F_o)$ . [c]  $wR_2 = [\sum[w(F_o^2 - F_c^2)^2]/\sum[w(F_o^2)^2]]^{1/2}$ ; see ref. [71].

Table 2. Selected distances ( $\text{\AA}$ ) and angles ( $^\circ$ ) for **4a** (major component).

Fe–C1	1.965(6)	Fe–C6	1.966(6)
Fe–C2	2.022(6)	Fe–C7	2.007(6)
Fe–C3	2.060(5)	Fe–C8	2.054(6)
Fe–C4	2.065(6)	Fe–C9	2.068(6)
Fe–C5	2.024(5)	Fe–C10	2.016(6)
C1–C11	1.540(7)	C11–C12	1.539(12)
C6–C12	1.544(7)	C1–C2	1.405(8)
C2–C3	1.408(9)	C3–C4	1.431(8)
C4–C5	1.406(9)	C1–C5	1.435(8)
C1–Fe–C6	88.6(3)	C11–C12–C6	114.5(8)
C1–C11–C12	105.9(8)	C10–Fe–C2	101.1(3)
C3–Fe–C9	120.1(3)	C4–Fe–C8	121.2(3)
C5–Fe–C7	101.1(3)	C1–C2–C3	108.6(6)
C2–C1–C5	108.0(5)	C4–C5–C1	107.4(5)
C2–C3–C4	107.6(5)	C5–C1–C11	120.8(8)
C2–C1–C11	130.1(8)	C10–C6–C12	114.3(8)
C7–C6–C12	136.0(8)		

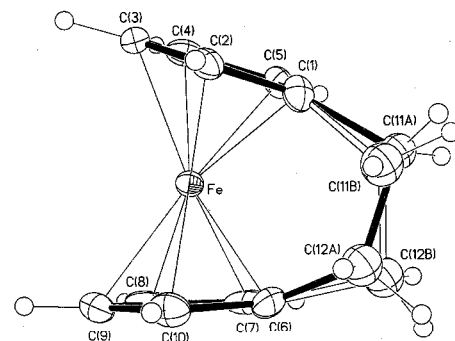


Figure 1. Molecular structure of **4a** (vibrational ellipsoids at the 25% probability level).

The most interesting structural feature of **4a** is the tilt of the virtually planar cyclopentadienyl ligands with respect to one another (Figure 1). The tilt angle of  $21.6(4)^\circ$  is comparable to that found for the silicon-bridged [1]ferrocenophane **1**

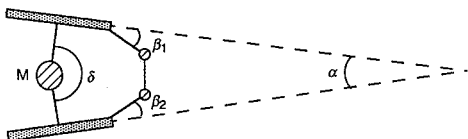


Figure 2. Definition of structural parameters for ferrocenophanes.

(20.8(5)°), slightly less than that present in the methylated hydrocarbon-bridged species **4c** (23(1)°). The degree of tilting in **4a** can also be appreciated by considering the  $C_{p_{\text{centroid}}}\text{-Fe-C}_{p_{\text{centroid}}}$  angle, which is 164.1(3)° compared with 180° in ferrocene, 163.4(6)° for **4c**, and 164.74(8)° in **1**. In **4c**, the displacement of the iron atom from the line joining the two centroids of the cyclopentadienyl ligands is greater than the value in **4a** (0.432(12) vs 0.225(7) Å). By contrast, the angles between the planes of the cyclopentadienyl ligands and the C(Cp)–C bonds ( $\beta$ ) in **4c** are 10.8(10)° and 8.9(13)°, which are smaller than in **4a** (20.1(3)° and 12.7(3)°), and angle  $\delta$  for **4a** (164.1(3)°) shows a considerably greater deviation from 180° than that for **3** ( $\delta = 176.48(3)^\circ$ ). In **4a**, the displacement of the iron atom from the line joining the two centroids of the cyclopentadienyl ligands (0.225(7) Å) is significantly greater than the value in **3** (0.027(3) Å). By contrast, the average angles between the planes of the cyclopentadienyl ligands and the C(Cp)–C bonds ( $\beta$ ) in **4a** are 20.1(3)° and 12.7(3)°, larger than the corresponding  $\beta$  angle in **3** (10.8(3)°). Interestingly, the  $C_2$  bridge in **4a** makes an angle of 18.4(1)° with the plane containing the centroids on the cyclopentadienyl rings and the iron atom and is therefore significantly more twisted than the disilane bridge in **3**, where the corresponding angle is 8.4(4)°.

It is also interesting to compare the structure of the recently reported hydrocarbon-bridged [2]ruthenocenophane  $[\text{Ru}(\eta\text{-C}_5\text{H}_4)_2(\text{CH}_2)_2]$  with that of its iron analogue **4a**.<sup>143, 561</sup> The larger size of the central ruthenium atom compared with iron results in drastic structural differences. The most interesting difference lies in the tilt angle  $\alpha$  between the planes of the cyclopentadienyl ligands in the ruthenium complex (29.6(5)°), which is ca. 8.0° greater than in the analogous iron species **4a** ( $\alpha = 21.6(4)^\circ$ ). In addition, the Cp–M–Cp angle  $\delta$  (M = Fe, Ru) for **4a** ( $\delta = 164.1(3)^\circ$ ) deviates less from 180° than that for the ruthenium analogue ( $\delta = 159.3(2)^\circ$ ). The displacement of the metal atom in the latter compound from the line joining the two centroids of the cyclopentadienyl ligands (0.321(5) Å) is greater than the corresponding value in **4a** (0.225(7) Å).

**Synthesis and structural characterization of the poly(ferrocenylethylene)s **5a** and **5b**:** Polymerization of **4a** and **4b** was achieved by heating these species in the melt at elevated temperatures in evacuated, sealed Pyrex tubes. In both cases the tube contents became molten and then rapidly more viscous, and eventually immobile. The polymeric product **5b** dissolved in THF and was isolated as a fibrous material by precipitation into methanol. By contrast, the unsubstituted polymer **5a** was found

to be essentially insoluble in organic solvents. The colours of **5a** and **5b** varied from mustard yellow to yellow-brown. The darker-coloured materials probably contained small amounts of thermal decomposition products (see below).

Although **5a** was insoluble, the polymeric nature of this material was suggested by its film-like appearance on the sides of the tube and by the identification of cyclic oligomers  $[\text{Fe}(\eta\text{-C}_5\text{-H}_4\text{CH}_2)_2]_x$  ( $x = 2\text{--}5$ ) in  $\text{CH}_2\text{Cl}_2$ -soluble extracts of the material by mass spectrometry. In addition, Soxhlet extraction with hot THF over 72 h produced a small amount of soluble material. Gel permeation chromatography (GPC) indicated that **5a** possessed a bimodal molecular weight distribution. The first fraction possessed an approximate weight average molecular weight ( $M_w$ ) of  $8.1 \times 10^4$  and a number average molecular weight ( $M_n$ ) of  $6.6 \times 10^4$  while the second, essentially oligomeric fraction was characterized by values of  $M_w = 4.8 \times 10^3$  and  $M_n = 3.5 \times 10^3$ . Because of the essentially insoluble nature of **5a**, this material was characterized by solid-state NMR. The solid-state  $^{13}\text{C}$  NMR spectrum displayed resonances consistent with the formation of a poly(ferrocenylethylene) (Figure 3) with broad resonances at  $\delta \approx 89\text{--}91$ ,  $68\text{--}72$  and  $35\text{--}38$  assigned to C(Cp-*ipso*), C( $\alpha$ ,  $\beta$ Cp), and  $\text{CH}_2\text{CH}_2$  bridging groups respectively. The yields of the poly(ferrocenylethylene)s **5a** and **5b** were virtually quantitative and no unreacted **4a** or **4b** was detected.

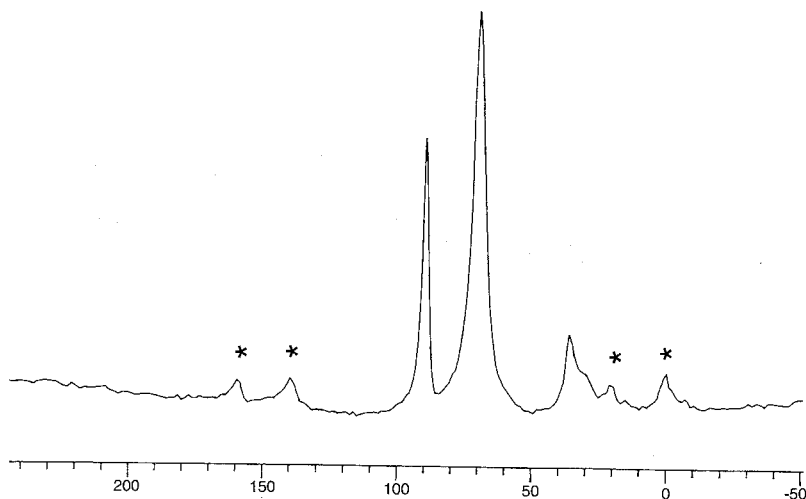


Figure 3. Solid-state  $^{13}\text{C}$  NMR spectrum of polymer **5a** (\* denotes spinning sidebands).

The poly(ferrocenylethylene) **5b**, which was readily soluble in organic solvents, was structurally characterized by multinuclear NMR spectroscopy, UV/vis spectroscopy and elemental analysis. In addition, the molecular weight distribution was analyzed by GPC. The  $^1\text{H}$  NMR spectra of **5b** (in  $\text{C}_6\text{D}_6$ ) showed a broad resonance for the cyclopentadienyl protons at  $\delta \approx 3.6\text{--}4.1$  and broad resonances assigned to the bridge protons and methyl groups associated with the cyclopentadienyl rings at  $\delta = 2.3\text{--}2.8$  and  $1.6\text{--}2.1$ , respectively. The integration ratio of these resonances was 6:4:6, which was consistent with the assigned structure. The  $^{13}\text{C}$  NMR spectrum for **5b** was complex, owing to the structural isomerism involving the methyl substituents attached to the cyclopentadienyl rings, but was also consistent with the assigned structure. Significantly, in the  $^{13}\text{C}$  NMR spectrum of **5b**, the resonance associated with the *ipso* carbon of the

cyclopentadienyl ring exhibits a slight highfield shift from  $\delta \approx 85.6\text{--}91.5$  in **4b** to  $83.3\text{--}88.5$  in **5b**, consistent with a structure in which the cyclopentadienyl rings are essentially parallel. The UV/visible data for polymer **5b** had a low-energy absorption at 440 nm ( $\epsilon_1 = 190\text{ M}^{-1}\text{ cm}^{-1}$ ) very similar to that of ferrocene ( $\lambda_{\text{max}} = 440\text{ nm}$ ;  $\epsilon_1 = 90\text{ M}^{-1}\text{ cm}^{-1}$ ); this suggests an essentially localized polymer backbone. GPC in THF indicated that **5b** possessed a bimodal molecular weight distribution. The first fraction had an approximate weight average molecular weight ( $M_w$ ) of  $9.6 \times 10^4$  and a number average molecular weight ( $M_n$ ) of  $8.6 \times 10^4$ , while the second, essentially oligomeric fraction was characterized by values of  $M_w = 4.8 \times 10^3$  and  $M_n = 3.5 \times 10^3$ .

The existence of a bimodal molecular weight distribution for polymer **5b** suggests the possibility that multiple mechanisms may operate during the thermal ROP of **4b**. In an attempt to examine the nature of the molecular weight distribution for **5b**, the polymerization of **4b** was examined more closely. Sealed Pyrex tubes containing **4b** were heated at  $300\text{ }^\circ\text{C}$  for intervals of 0–2.5 h and the contents of each tube were examined by GPC. Analysis of a tube heated for 30 min (at which time the tube contents were viscous but mobile) showed that the polymer present possessed an approximate weight average molecular weight ( $M_w$ ) of  $8.0 \times 10^4$  and a number average molecular weight ( $M_n$ ) of  $6.6 \times 10^4$  with no substantial lower molecular weight oligomeric fraction. Analysis of the contents of the tubes which had been heated for 45 min or more (after which time the tube contents were immobile) showed the aforementioned characteristic bimodal molecular weight distribution. In order to determine whether the lower molecular weight fraction arises as a result of thermal decomposition of the polymer, a tube containing a purified sample of polymer **5b** was heated for 1 h at  $300\text{ }^\circ\text{C}$ . Analysis of the tube contents by GPC showed no change in molecular weight or in the molecular weight distribution. Thermogravimetric analysis of polymer **5b** supports this finding, as this material is stable to weight loss up to ca.  $375\text{ }^\circ\text{C}$  (see below), which is above the ROP temperature. These results provide support for the tentative postulate of two different polymerization mechanisms.

**Attempted transition-metal-catalyzed ROP of 4a:** Recently, in an effort to induce strained silicon-bridged [1]ferrocenophanes such as **1** to undergo ROP under milder conditions, the use of various transition-metal catalysts was explored. This resulted in the formation of high molecular weight poly(ferrocenylsilane)s (e.g. **2**) at room temperature.<sup>[24, 57, 58]</sup> Attempts to extend this chemistry to similarly strained hydrocarbon-bridged [2]metallocenophane systems such as **4a**, however, were, not surprisingly, unsuccessful. Solutions of **4a** (in  $\text{C}_6\text{D}_6$ ) were treated with bis(cyclooctene)rhodium(i) chloride dimer, and the mixture was stirred under nitrogen with constant monitoring by  $^1\text{H}$  NMR spectroscopy. Analysis of this mixture after 48 h by both  $^1\text{H}$  NMR spectroscopy and GPC showed only the presence of the starting compound **4a** and no signs of oligomeric or polymeric material. Similar results were obtained with  $\text{PtCl}_2$  and platinum divinyltetramethyldisiloxane complex as the catalysts.

**Thermal transition behaviour and morphology of the poly(ferrocenylethylene)s 5a and 5b:** In order to obtain information on the

conformational flexibility and morphology of the poly(ferrocenylethylene)s, the thermal transition behaviour of **5a** and **5b** was investigated. Whereas differential scanning calorimetry (DSC) showed no evidence for melting transitions for polymer **5b**, a large melting endotherm ( $T_m$ ) at  $241\text{ }^\circ\text{C}$  was detected with the corresponding recrystallization exotherm at  $191\text{ }^\circ\text{C}$  detected on cooling (Figure 4) for polymer **5a**. For polymer **5b**, only a

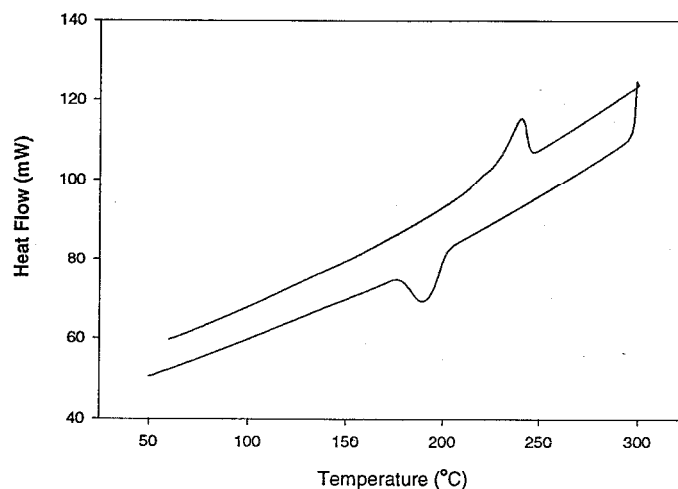


Figure 4. DSC thermogram for polymer **5a** (scan rate of  $10\text{ }^\circ\text{C min}^{-1}$ ).

glass transition with very small change in heat capacity was detected at ca.  $65\text{ }^\circ\text{C}$ , and no apparent  $T_g$  was observed for polymer **5a**. Comparison of the glass-transition data with data for polyethylene, which has a  $T_g$  value of  $-120\text{ }^\circ\text{C}$ , reveals that the inclusion of ferrocene into the polyethylene backbone decreases the skeletal flexibility. Also, comparison of the glass transition temperature for the poly(ferrocenylethylene) **5b** with that for poly(vinylferrocene) ( $T_g = 184\text{ }^\circ\text{C}$ ),<sup>[59]</sup> where ferrocene is present as a side group, indicates that the incorporation of a ferrocenyl moiety into the backbone decreases the conformational flexibility less dramatically.

The morphology of the poly(ferrocenylethylene)s was also examined by wide-angle X-ray scattering (WAXS) at  $25\text{ }^\circ\text{C}$ . The WAXS scattering pattern for **5a** showed significant order, with a sharp peak corresponding to a  $d$  spacing of  $5.14\text{ \AA}$  (Figure 5). Scattering patterns for **5b** were broad with no significant signs of long-range order and displayed a broad peak corresponding to a  $d$  spacing of  $6.18\text{ \AA}$  superimposed on an amorphous halo (Figure 5, inset).

#### Thermal stability of the poly(ferrocenylethylene)s 5a and 5b:

**a) Thermogravimetric analysis:** Thermogravimetric analysis (TGA) studies of the polymer **5b** under  $\text{N}_2$  at a heating rate of  $10\text{ }^\circ\text{C min}^{-1}$  showed that this material was stable to weight loss up to ca.  $375\text{ }^\circ\text{C}$  (Figure 6). Above this temperature two distinct weight-loss processes were detected. An initial weight loss of approximately 48% occurred between  $375\text{ }^\circ\text{C}$  and  $450\text{ }^\circ\text{C}$ , with a subsequent weight loss of approximately 20% observed between  $450\text{ }^\circ\text{C}$  and  $500\text{ }^\circ\text{C}$ . Further thermolysis up to  $1000\text{ }^\circ\text{C}$  led to very little change in mass. The final char yield for this polymer was 32%. Analogous thermolysis studies on polymer **5a** showed similar behaviour with a higher final char yield of 50%.

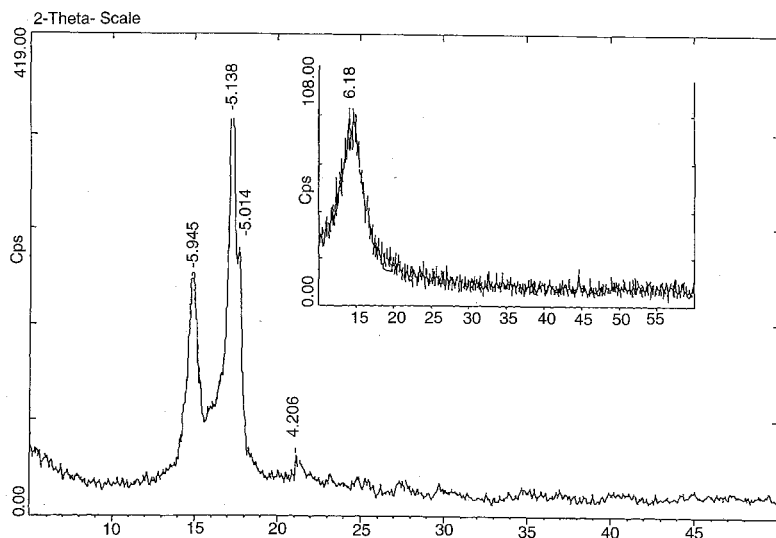


Figure 5. Wide-angle X-ray scattering pattern for polymers **5a** and **5b** (inset) at 25°C.

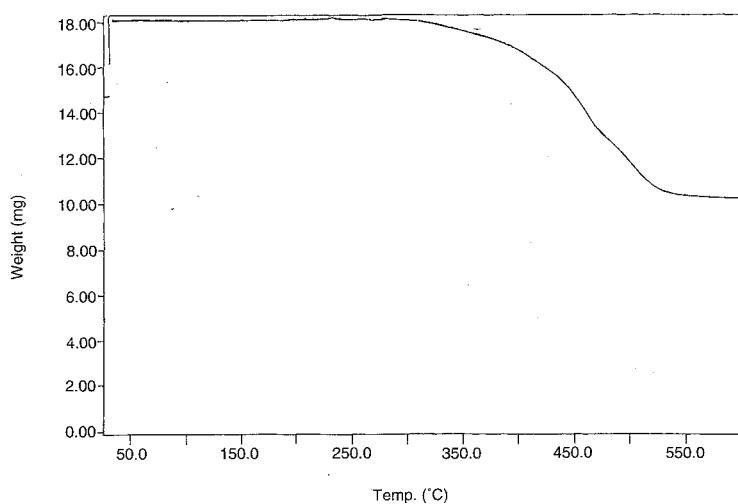


Figure 6. Thermogravimetric analysis trace for polymer **5b** obtained at 10°C min<sup>-1</sup> under N<sub>2</sub>.

*b) Pyrolysis studies in a tube furnace:* In order to investigate the thermolysis of poly(ferrocenylethylene)s in more detail, studies in a tube furnace were carried out. Polymer **5b** was chosen for this work because it could be purified more thoroughly than **5a**, since the latter material is essentially insoluble in organic solvents. Pyrolysis of **5b** was carried out under N<sub>2</sub> with a 1 h ramp from room temperature to 600°C and subsequent thermolysis for 4 h at this temperature. Ceramics were obtained as black, lustrous materials in yields of ca. 30%. Concurrent with the onset temperature for weight loss by TGA (375°C), the formation of a red-orange oil was observed on the cooler section of the quartz tube downstream from the polymer sample.

*c) Characterization of the pyrolysis products:* The solid pyrolysis product **6b**, formed during the thermolysis of **5b** at 600°C, was readily attracted to a bar magnet and was further investigated by X-ray photoelectron spectroscopy (XPS), high-resolution scanning electron microscopy (SEM) with energy dispersive X-ray microanalysis (EDX) and backscattered electron imaging

(BEI), Mössbauer spectroscopy, magnetization measurements, and X-ray powder diffraction (XRD).

Analysis of the ceramic **6b** by XPS indicated the presence of a surface primarily containing carbon (ca. 87%) with some oxygen (ca. 11%). The presence of oxygen was also noted for the ceramics derived from the pyrolysis of poly(ferrocenylsilane)s and may arise from workup of the pyrolysis products in air.<sup>[22,29]</sup> Analysis of the bulk of the sample by SEM-EDX, with samples of polymer **5b** for compositional comparisons, showed an iron:carbon:oxygen ratio of approximately 72:24:4. Interestingly, the material was not homogeneous and small regions of higher oxygen concentration (iron:carbon:oxygen ratio = 70:5:25) were also present (see Figure 7).

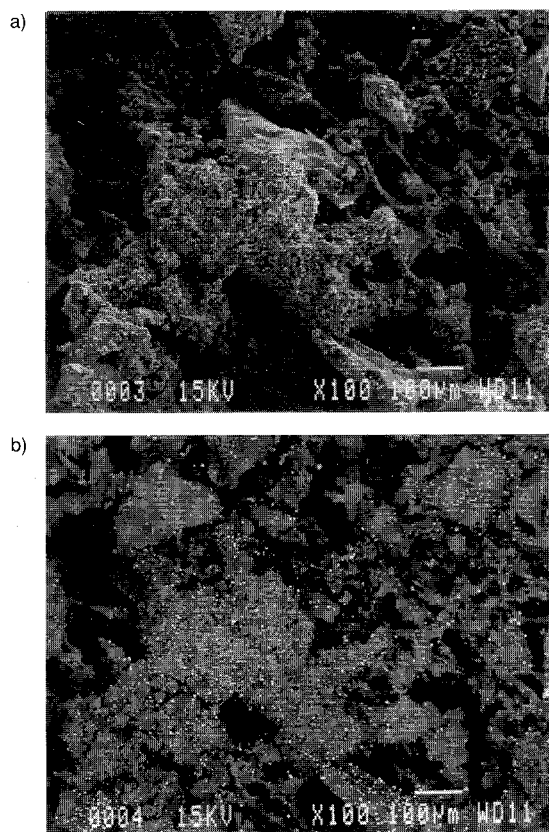


Figure 7. a) Scanning electron micrograph of ceramic **6b** at ×100 magnification. b) Back-scattered electron image of ceramic **6b** at ×100 magnification.

The magnetic properties of the ceramic **6b** were studied by Mössbauer spectroscopy and magnetization measurements. The <sup>57</sup>Fe Mössbauer spectrum of **6b** confirmed the presence of magnetic iron sites with a characteristic six-line spectrum arising from the lifting of the degeneracy of the  $I = \pm 1/2$  and  $\pm 3/2$  states. A study of the magnetization of **6b** as a function of applied field gave a hysteresis curve characteristic of a soft ferromagnetic material. A study of **6b** by powder XRD indicated the presence of significant amounts of  $\alpha$ -Fe crystallites (sharp peaks at  $d$  spacings of 2.02(5), 1.43(3) and 1.17(3) Å) together with several broadened peaks of low intensity (Figure 8). Simi-



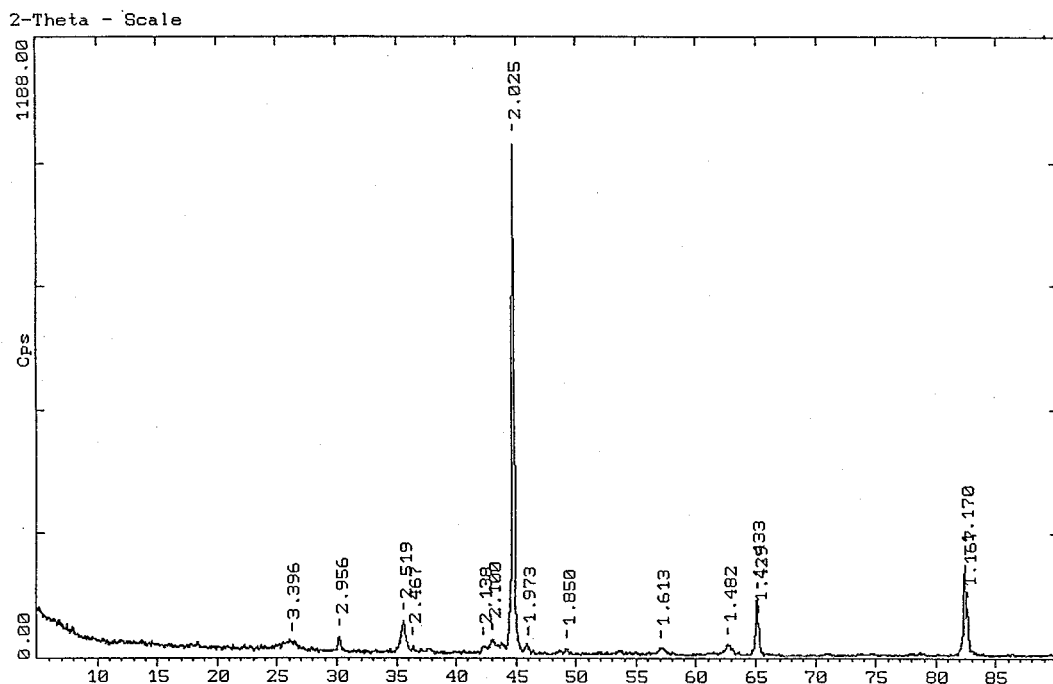
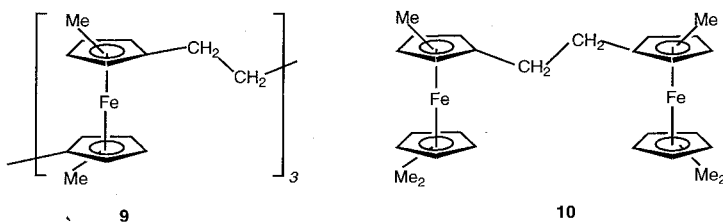


Figure 8. X-ray diffraction pattern for ceramic **6b** at 25°C.

lar behaviour has been noted for the ceramics derived from the pyrolysis of poly(ferrocenylsilane)s, where much higher ceramic yields have been achieved.<sup>[21,22,29]</sup>

The liquid produced during the pyrolysis of **5b** was collected in dichloromethane solvent and was analyzed by mass spectrometry. The peaks were tentatively assigned to cyclic trimer  $[\text{Fe}(\eta\text{-C}_5\text{H}_3(\text{CH}_3)\text{CH}_2)_2]_3$  (**9**) and the linear methylated compounds  $[\text{Fe}\{\eta\text{-C}_5\text{H}_3\text{Me}_2\}\{\eta\text{-C}_5\text{H}_3(\text{Me})\}(\text{CH}_2)]_2$  (**10**). Cyclic depolymerization products have been previously detected when poly(ferrocenyldimethylsilane) (**2**) is heated at elevated temperatures.<sup>[22,29]</sup>



**Cyclic voltammetry studies of poly(ferrocenylethylene) **5b**:** Previous cyclic voltammetric studies focussing on the electrochemical behaviour of poly(ferrocenylsilane)s such as **2** have shown that there are electronic interactions between the metal atoms of the main chain in these polymers. Thus, poly(ferrocenyldimethylsilane) **2** exhibits two reversible oxidation waves with a redox coupling  $\Delta E_{1/2}$  of 0.25 V.<sup>[11,25]</sup> To determine whether similar interactions would be present with other elements instead of silicon, cyclic voltammograms of the poly(ferrocenylethylene) **5b** in  $\text{CH}_2\text{Cl}_2$  solutions were recorded at a variety of scan rates (Figure 9). Two reversible oxidation waves were observed as a result of slight electronic communication between metal centres along the polymer chain. Initial oxidation of alternating iron

sites at a potential of  $-0.25$  V was found to increase the oxidation potential of a neighbouring iron site to  $-0.16$  V. The presence of a more insulating hydrocarbon bridge dampens electronic interaction between metal centres along the polymer backbone in polymer **5b**, which has a smaller redox coupling ( $\Delta E_{1/2}$ ) of 0.09 V. For **5b**, plots of current vs. square root of scan rate were linear over the range of scan rates employed ( $50\text{--}2000$   $\text{mVs}^{-1}$ ) for both oxidation waves; this indicated that the electron transfer was essentially diffusion-controlled (see inset in Figure 9). Electrochemical studies of hydrocarbon-bridged biferrocene systems, such as the ethane-bridged dimer  $\text{Fc}-(\text{CH}_2)_2\text{-Fc}$ , have shown contrasting behaviour; this compound exhibits only one reversible oxidation wave at  $E_{1/2} = 0.37$  V vs. SCE.<sup>[60]</sup>

hydrocarbon-bridged biferrocene systems, such as the ethane-bridged dimer  $\text{Fc}-(\text{CH}_2)_2\text{-Fc}$ , have shown contrasting behaviour; this compound exhibits only one reversible oxidation wave at  $E_{1/2} = 0.37$  V vs. SCE.<sup>[60]</sup>

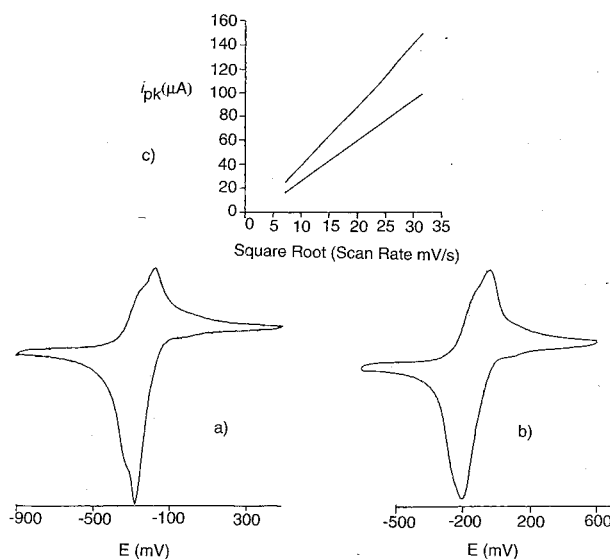


Figure 9. Cyclic voltammograms of polymer **5b** in  $\text{CH}_2\text{Cl}_2$  obtained at scan rate of a) 50 and b) 250  $\text{mVs}^{-1}$  at 25°C referenced to the ferrocene/ferrocenium couple at  $E = 0.0$  mV. Also shown are plots of  $i_{pk}$  vs. the square root of the scan rate for the oxidation peaks observed for **5b**.

**Mössbauer spectroscopic studies of poly(ferrocenylethylene) **5b**:** A room-temperature Mössbauer spectrum of an air-oxidized sample of **5b** was obtained in order to probe the nature of the possible different iron sites in the resulting polymer (Figure 10). The Mössbauer spectrum for the oxidized poly(ferrocenylethylene) **5b** displayed a pair of doublets, with the outer doublet

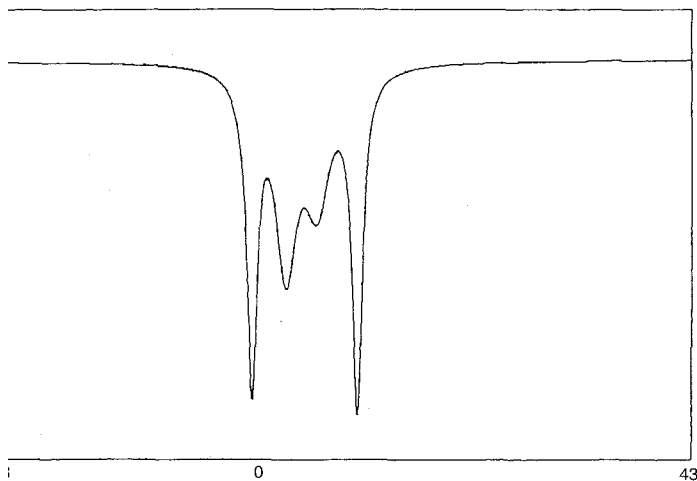


Figure 10. Mössbauer spectrum of partially oxidized **5b** at 25°C.

having an isomer shift ( $\delta$ ) of  $0.382 \text{ mm s}^{-1}$  and quadrupole splitting value ( $\Delta E_q$ ) of  $2.33 \text{ mm s}^{-1}$ , while the inner doublet displayed a  $\delta$  of  $0.31 \text{ mm s}^{-1}$  and  $\Delta E_q$  of  $0.69 \text{ mm s}^{-1}$ , characteristic of  $\text{Fe}^{\text{II}}$  and  $\text{Fe}^{\text{III}}$  sites, respectively. This implies that the oxidized **5b** has a localized electronic structure on the Mössbauer timescale ( $10^{-7} \text{ s}$ ).

**Characterization of the oxidation products from the reaction of the poly(ferrocenylethylene) **5b** with TCNE:** The preparation of magnetic materials derived from polymer **5b** was somewhat complicated by the presence of very small but variable quantities of magnetic impurities in the polymer. These impurities are presumably pyrolysis products formed during the high temperatures (ca.  $300^\circ\text{C}$ ) required for the synthesis of **5b**.

The unoxidized polymer (even the purest material obtained) showed a characteristic, very unsymmetrical ESR signal at an apparent  $g$  value of ca. 2 at room temperature, but gave no discernible ESR signal below ca. 100 K. Magnetic measurements of samples with greater impurity levels indicate a drop in susceptibility below ca. 130 K; the magnetic susceptibility at low temperature is very small. These results are consistent with the presence of non-ferrocene/ferrocenium-derived iron species that undergo a spin crossover at ca. 130 K. The proportion of this impurity is very small, as it does not affect the elemental analysis of the neutral polymer; presumably the species responsible has a rather large moment.

Addition of a dichloromethane solution of one equivalent of TCNE to a dichloromethane solution of **5b** resulted in the formation of two products: a black insoluble material (**11**, ca. 40%) was collected by filtration, and a green precipitate (**12**, ca. 60%) was obtained by addition of diethyl ether to the filtered dichloromethane solution. Elemental analyses were consistent with stoichiometries close to  $\text{5b} \cdot [\text{TCNE}]_n$  for each product.

The only multiple-bond stretching bands observed in the IR spectrum of a nujol mull of **11** were broad intense features centred at  $2153$  and  $2198 \text{ cm}^{-1}$ ; these are indicative of reduced TCNE but at somewhat higher frequency than the isolated  $\text{TCNE}^-$  anion.<sup>[61–63]</sup> A plausible explanation is that the material includes stacks of planar TCNE molecules, which are partially reduced. Compound **11** was also investigated by ESR spectroscopy and SQUID magnetometry. Unfortunately, the

magnetic impurity present in the unoxidized polymer appears to end up in this reaction product. Thus, the room-temperature ESR spectrum revealed the characteristic spectrum of the unoxidized polymer, upon which is superimposed a sharp isotropic resonance with  $g = 2.00$ , presumably arising from the cyanocarbon anions. At low temperatures the isotropic resonance completely dominated any signal from the impurity in the polymer. In addition, an axially symmetric ferrocenium spectrum was observed characterized by  $g_{\perp} = 1.70$  and  $g_{\parallel} = 3.76$ . These values are typical for substituted ferrocenium species.<sup>[64–66]</sup> This spectrum is surprisingly sharp given that the sample was a solid and that ferrocenium ions with slightly different substitution patterns and, therefore, with slightly different  $g$  values, are expected to be present, owing to the variation in the positions of the methyl groups on the cyclopentadienyl rings. The magnetic susceptibility data could not be fitted to the Curie–Weiss law. As magnetic impurities were shown to be present by ESR, no further analysis of the magnetic data was undertaken.

A nujol mull of the soluble material **12** shows IR bands at  $2148$ ,  $2199$  and  $2218 \text{ cm}^{-1}$ , the middle band being particularly intense. This is similar to the spectrum observed for the  $\text{TCNE}_2^-$  anion,<sup>[67]</sup> although the bands are spread over a wider range of frequencies in **12** and, on average, are at somewhat higher frequency. A very similar IR spectrum is observed in dichloromethane solution, indicating the oligomeric anions do not dissociate in solution. Room-temperature ESR spectra of **12**, either in the solid state or in dichloromethane solution, showed a very poorly resolved isotropic resonance with a  $g$  value of ca. 2. The characteristic lineshape of the impurity in the unoxidized polymer was not observed; this was taken to indicate that this product is essentially free of the magnetic impurity. The low intensity of the room-temperature radical signal, when compared with spectra of other salts of paramagnetic cyanocarbon species, suggests few anions are paramagnetic. Low-temperature spectra showed the isotropic radical resonance and a ferrocenium spectrum with  $g$  values almost identical to those from the ferrocenium spectrum of **11**. Spectra were acquired both in dichloromethane and with solid samples; although the solution/glass spectra were slightly sharper, the spectra were otherwise very similar, consistent with the anions being unchanged when the material is dissolved. Solid-state magnetic susceptibility measurements were made between 5 and 250 K. The data were fitted to the Curie–Weiss law (80–250 K) with a Weiss constant  $\Theta$  of  $-11.6 \text{ K}$  (Figure 11). This value is indicative of significant antiferromagnetic interactions. The magnetic moment is ca.  $1.7 \mu_{\text{B}}$  per iron atom, although this value depends

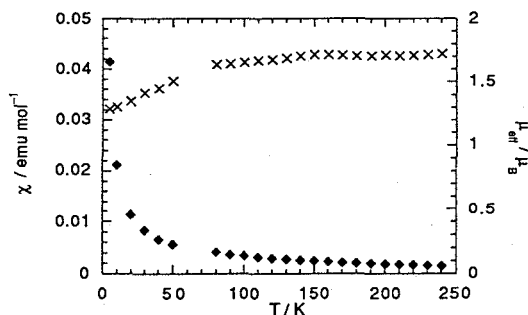


Figure 11. Variation of molar magnetic susceptibility per Fe ( $\chi$ , ♦) and effective magnetic moment ( $\mu_{\text{eff}}$ , ×) with temperature ( $T$ ) for **12**.

greatly upon the accuracy of the iron analysis. For a fully oxidized polymer with diamagnetic counterions, one would expect an effective magnetic moment of  $2.25 \mu_B$ , if  $\langle g \rangle = 2.60$  as determined by ESR. Below ca. 70 K the plot of reciprocal susceptibility against temperature is no longer linear, and the derived magnetic moment falls to  $1.2 \mu_B$  (Figure 11). This is also consistent with the presence of substantial antiferromagnetic interactions in the material; however, the data show no transition to an ordered antiferromagnetic state.

The formation of two distinct products of similar composition in this reaction is not especially surprising. The products of reactions involving cyanocarbon anions often give more than one product.<sup>[68–70]</sup> Thus, for example, Ward et al. were able to isolate both green TCNQ<sup>−</sup> (TCNQ = 7,7,8,8-tetracyano-*p*-quinodimethane) and purple TCNQ<sub>2</sub><sup>2−</sup> salts of the [Cp\**Ru*-(C<sub>6</sub>Me<sub>6</sub>)]<sup>+</sup> cation from a single reaction mixture.<sup>[70]</sup> The origin of the antiferromagnetic interactions in **12** is unknown. However, it is possible that the packing requirements of the cyanocarbon counterions cause ferrocenium ions to be in close proximity with one another.

### Summary

The poly(ferrocenylethylene)s [Fe( $\eta$ -C<sub>5</sub>H<sub>3</sub>RCH<sub>2</sub>)<sub>2</sub>]<sub>*n*</sub> **5a** and **5b** (**a**: R = H, **b**: R = Me) have been prepared by the thermal ring-opening polymerization of the corresponding strained hydrocarbon-bridged [2]ferrocenophanes [Fe( $\eta$ -C<sub>5</sub>H<sub>3</sub>RCH<sub>2</sub>)<sub>2</sub>]. The molecular weight distribution for polymer **5b** was found to be bimodal in nature with a high molecular weight fraction with  $M_w \approx 10^5$  and a low molecular weight fraction with  $M_w \approx 10^3$ . This may be the result of the action of two different polymerization mechanisms. A UV/visible spectrum of polymer **5b** was consistent with a localized structure for the polymer backbone. The electrochemical behaviour of the polymer **5b** was examined by cyclic voltammetry, which revealed that this polymer undergoes two reversible, closely spaced oxidations in CH<sub>2</sub>Cl<sub>2</sub> solutions at  $-0.25$  and  $-0.16$  V, with a redox coupling  $\Delta E_{1/2}$  of approximately 0.09 V, indicative of only a small interaction between the iron centres. Studies by TGA indicated that poly(ferrocenylethylene)s are thermally stable to weight loss to about 375°C under dinitrogen, and at more elevated temperatures yield ferromagnetic ceramic products.

The reaction of the poly(ferrocenylethylene) **5b** with TCNE gave a mixture of two products, **11** and **12**, which differ in their solubilities and the degree of oligomerization of the TCNE<sub>*x*</sub><sup>−</sup> counterions. Magnetic characterization of **11** was complicated by the presence of small amounts of magnetic impurities present in the neutral polymer. Nevertheless, solid-state magnetic susceptibility measurements show significant antiferromagnetic interactions in **12**.

**Acknowledgments:** I. M. thanks the Ontario Center for Materials Research (OCMR) and the Petroleum Research Fund (PRF), administered by the American Chemical Society (ACS), for funding, and the Alfred P. Sloan Foundation for a Research Fellowship (1994–1998). J. M. N. thanks the University of Toronto for a Simcoe Fellowship, P. N. thanks the Natural Sciences and Engineering Research Council of Canada (NSERC) for a post-doctoral fellowship, and H. R. is grateful to the Deutscher Akademischer Austauschdienst (DAAD) for an overseas exchange award. D. O'H. would like to acknowledge EPSRC for financial support and a studentship (S. B.),

and the Royal Society of Chemistry (RSC) Dalton Division for the Sir Edward Franklin Fellowship. The authors also thank Prof. R. H. Morris for the use of the electrochemical equipment and Prof. G. Ozin for the use of the Mössbauer spectrometer.

Received: August 8, 1996 [F 438]

- [1] a) *Inorganic Materials* (Eds.: D. W. Bruce, D. O'Hare), Wiley, Chichester, **1992**; b) *Extended Linear Chain Compounds*, Vols. 1–3 (Ed.: J. S. Miller), Plenum, New York, **1982**; c) S. L. Ingham, N. J. Long, *Angew. Chem.* **1994**, *106*, 1847; *Angew. Chem. Int. Ed. Engl.* **1994**, *33*, 1752; d) L. Oriol, J. L. Serrano, *Adv. Mater.* **1995**, *7*, 348; e) N. G. Connelly, W. E. Geiger, *Adv. Organomet. Chem.* **1984**, *23*, 1; f) N. G. Connelly, W. E. Geiger, *ibid.* **1985**, *24*, 87.
- [2] D. O'Hare, *Chem. Soc. Rev.* **1992**, 121.
- [3] a) J. E. Mark, H. R. Allcock, R. West, *Inorganic Polymers*, Prentice Hall, **1992**; b) C. U. Pittman, C. E. Carraher, J. R. Reynolds, in *Encyclopedia of Polymer Science and Engineering* (Eds.: H. F. Mark, N. M. Bikales, C. G. Overberger, G. Menges), Wiley, New York, **1989**, Vol. 10, p. 541; c) J. E. Sheats, C. E. Carraher, C. U. Pittman, *Metal-Containing Polymeric Systems*, Plenum, New York, **1985**; d) *Inorganic and Metal-Containing Polymeric Materials* (Eds.: J. E. Sheats, C. E. Carraher, C. U. Pittman, M. Zeldin, B. Currell), Plenum, New York, **1989**; e) *Inorganic and Organometallic Polymers* (Eds.: M. Zeldin, K. Wynne, H. R. Allcock), ACS, Washington D. C., **1988**, Vol. 360.
- [4] a) J. S. Miller, A. J. Epstein, W. M. Reiff, *Acc. Chem. Res.* **1988**, *21*, 114; b) J. S. Miller, A. J. Epstein, W. M. Reiff, *Chem. Rev.* **1988**, *88*, 201.
- [5] I. Manners, *Angew. Chem.* **1996**, *108*, 1712; *Angew. Chem. Int. Ed. Engl.* **1996**, *35*, 1602.
- [6] a) H. M. Nugent, M. Rosenblum, P. Klemarczyk, *J. Am. Chem. Soc.* **1993**, *115*, 3848; b) M. Rosenblum, *Adv. Mater.* **1994**, *6*, 159; c) M. Rosenblum, H. M. Nugent, K.-S. Jang, M. M. Labes, W. Cahalane, P. Klemarczyk, W. M. Reiff, *Macromolecules* **1995**, *28*, 6330; d) R. Arnold, S. A. Matchett, M. Rosenblum, *Organometallics* **1988**, *7*, 2261; e) B. M. Foxman, M. Rosenblum, *ibid.* **1993**, *12*, 4805; f) B. M. Foxman, D. A. Gronbeck, M. Rosenblum, *J. Organomet. Chem.* **1991**, *413*, 287.
- [7] a) P. F. Brandt, T. B. Rauchfuss, *J. Am. Chem. Soc.* **1992**, *114*, 1926; b) C. P. Galloway, T. B. Rauchfuss, *Angew. Chem.* **1993**, *105*, 1407; *Angew. Chem. Int. Ed. Engl.* **1993**, *32*, 1319; c) D. L. Compton, T. B. Rauchfuss, *Organometallics* **1994**, *13*, 4367; d) D. L. Compton, P. F. Brandt, T. B. Rauchfuss, D. F. Rosenbaum, C. F. Zukoski, *Chem. Mater.* **1995**, *7*, 2342.
- [8] C. E. Stanton, T. R. Lee, R. H. Grubbs, N. S. Lewis, J. K. Pudelski, M. R. Callstrom, M. S. Erickson, M. L. McLaughlin, *Macromolecules* **1995**, *28*, 8713.
- [9] a) M. E. Wright, E. G. Toplikar, H. S. Lackritz, J. T. Kerney, *Macromolecules* **1994**, *27*, 3016; b) B. Alonso, M. Morán, C. Casado, F. Lobete, J. Losada, I. Cuadrado, *Chem. Mater.* **1995**, *7*, 1440.
- [10] O. Nuyken, T. Pöhimann, M. Herberhold, *Macromol. Rep.* **1992**, *A29*, 211.
- [11] D. A. Foucher, B.-Z. Tang, I. Manners, *J. Am. Chem. Soc.* **1992**, *114*, 6246.
- [12] D. A. Foucher, I. Manners, *Makromol. Chem. Rapid Commun.* **1993**, *14*, 63.
- [13] C. H. Honeyman, D. A. Foucher, F. Y. Dahmen, R. Rulkens, A. J. Lough, I. Manners, *Organometallics* **1995**, *14*, 5503.
- [14] J. K. Pudelski, D. P. Gates, R. Rulkens, A. J. Lough, I. Manners, *Angew. Chem.* **1995**, *107*, 1633; *Angew. Chem. Int. Ed. Engl.* **1995**, *34*, 1506.
- [15] R. Rulkens, A. J. Lough, I. Manners, *Angew. Chem.* **1996**, *108*, 1929; *Angew. Chem. Int. Ed. Engl.* **1996**, *35*, 1805.
- [16] For a recent Highlights article on strained metallocenophanes, see M. Herberhold, *Angew. Chem.* **1995**, *107*, 1985; *Angew. Chem. Int. Ed. Engl.* **1995**, *34*, 1837.
- [17] D. A. Foucher, R. Ziembinski, B.-Z. Tang, P. M. Macdonald, J. Massey, C. R. Jaeger, G. J. Vancso, I. Manners, *Macromolecules* **1993**, *26*, 2878.
- [18] D. A. Foucher, C. H. Honeyman, J. M. Nelson, B.-Z. Tang, I. Manners, *Angew. Chem.* **1993**, *105*, 1843; *Angew. Chem. Int. Ed. Engl.* **1993**, *32*, 1709.
- [19] D. A. Foucher, R. Ziembinski, R. Petersen, J. Pudelski, M. Edwards, Y. Ni, J. Massey, C. R. Jaeger, G. J. Vancso, I. Manners, *Macromolecules* **1994**, *27*, 3992.
- [20] J. K. Pudelski, I. Manners, *J. Am. Chem. Soc.* **1995**, *117*, 7265.
- [21] J. K. Pudelski, R. Rulkens, D. A. Foucher, A. J. Lough, P. M. Macdonald, I. Manners, *Macromolecules* **1995**, *28*, 7301.
- [22] R. Petersen, D. A. Foucher, B.-Z. Tang, A. J. Lough, N. P. Raju, J. E. Greedan, I. Manners, *Chem. Mater.* **1995**, *7*, 2045.
- [23] J. Rasburn, R. Petersen, T. Jahr, R. Rulkens, I. Manners, G. J. Vancso, *Chem. Mater.* **1995**, *7*, 871.
- [24] D. L. Zechel, K. C. Hultzsich, R. Rulkens, D. Balaishis, Y. Ni, J. K. Pudelski, A. J. Lough, I. Manners, *Organometallics* **1996**, *15*, 1972.
- [25] I. Manners, *Adv. Organomet. Chem.* **1995**, *37*, 131.
- [26] a) M. T. Nguyen, A. F. Diaz, V. V. Dement'ev, K. H. Pannell, *Chem. Mater.* **1993**, *5*, 1389; b) K. H. Pannell, V. V. Dement'ev, H. Li, F. Cervantes-Lee, M. T. Nguyen, A. F. Diaz, *Organometallics* **1994**, *13*, 3644.
- [27] M. Hmyene, A. Yasser, M. Escorne, A. Percheron-Guegan, F. Garnier, *Adv. Mater.* **1994**, *6*, 564.

- [28] M. J. Drewitt, S. Barlow, D. O'Hare, J. M. Nelson, P. Nguyen, I. Manners, *Chem. Commun.* **1996**, 2153.
- [29] B.-Z. Tang, R. Petersen, D. A. Foucher, A. J. Lough, N. Coombs, R. Sodhi, I. Manners, *J. Chem. Soc. Chem. Commun.* **1993**, 523.
- [30] S. Barlow, A. L. Rohl, D. O'Hare, *Chem. Commun.* **1996**, 257.
- [31] S. Barlow, A. L. Rohl, S. Shi, C. M. Freeman, D. O'Hare, *J. Am. Chem. Soc.* **1996**, *118*, 7578.
- [32] H. Stoeckli-Evans, A. G. Osborne, R. H. Whiteley, *Helv. Chim. Acta* **1976**, *59*, 2402.
- [33] H. Stoeckli-Evans, A. G. Osborne, R. H. Whiteley, *J. Organomet. Chem.* **1980**, *194*, 91.
- [34] D. Seyferth, H. P. Withers, *Organometallics* **1982**, *1*, 1275.
- [35] I. R. Butler, W. R. Cullen, F. W. B. Einstein, S. J. Rettig, A. J. Willis, *Organometallics* **1983**, *2*, 128.
- [36] M. Edwards, D. A. Foucher, A. J. Lough, I. Manners, *Z. Kristallogr.* **1995**, *210*, 865.
- [37] J. K. Pudelski, D. A. Foucher, C. H. Honeyman, A. J. Lough, I. Manners, S. Barlow, D. O'Hare, *Organometallics* **1995**, *14*, 2470.
- [38] W. Finekh, B.-Z. Tang, D. A. Foucher, D. B. Zamble, R. Ziembinski, A. Lough, I. Manners, *Organometallics* **1993**, *12*, 823.
- [39] After the publication of ref. [38], Pannell and co-workers also reported the structure of **3**: V. V. Dement'ev, F. Cervantes-Lee, L. Parkanyi, H. Sharma, K. H. Pannell, M. T. Nguyen, A. Diaz, *Organometallics* **1993**, *12*, 1983.
- [40] M. Burke Laing, K. N. Truethood, *Acta. Crystallogr.* **1965**, *19*, 373.
- [41] J. M. Nelson, H. Rengel, I. Manners, *J. Am. Chem. Soc.* **1993**, *115*, 7035.
- [42] Alternative names for polymers such as **5a** and **5b** include poly(ferrocenylene-ethylene)s, poly(ferrocenyleneethane)s and poly(ferrocenediethylene)s. A similar nomenclature situation arises for polymers such as **2**.
- [43] J. M. Nelson, A. J. Lough, I. Manners, *Angew. Chem.* **1995**, *106*, 1019; *Angew. Chem. Int. Ed. Engl.* **1994**, *33*, 989.
- [44] D. A. Foucher, R. Ziembinski, R. Rulkens, J. M. Nelson, I. Manners, in *Inorganic and Organometallic Polymers II* (Eds.: P. Wisian-Neilson, H. R. Allcock, K. J. Wynne), ACS, Washington D. C., **1994**, Vol. 572, p. 442.
- [45] J. K. Pudelski, D. A. Foucher, C. H. Honeyman, P. M. Macdonald, I. Manners, S. Barlow, D. O'Hare, *Macromolecules* **1996**, *29*, 1894.
- [46] C. S. Cundy, C. Eaborn, M. F. Lappert, *J. Organomet. Chem.* **1972**, *44*, 291.
- [47] S. Collins, Y. Hóng, N. J. Taylor, *Organometallics* **1990**, *9*, 2695.
- [48] E. W. Neuse, H. Rosenberg, *J. Macromol. Sci. Rev. Macromol. Chem.* **1970**, *C4*, 1.
- [49] E. W. Neuse, E. Quo, *J. Polym. Sci.* **1965**, *A3*, 1499.
- [50] A. Lüttinghaus, W. Kullick, *Angew. Chem.* **1958**, *70*, 438.
- [51] H. L. Lentzner, W. E. Watts, *Chem. Commun.* **1970**, 906.
- [52] H. L. Lentzner, W. E. Watts, *Tetrahedron* **1971**, *27*, 4343.
- [53] A. G. Osborne, R. H. Whiteley, R. E. Meads, *J. Organomet. Chem.* **1980**, *193*, 345.
- [54] R. B. Abramovitch, J. J. Atwood, M. L. Good, B. A. Lampert, *Inorg. Chem.* **1975**, *14*, 3085.
- [55] K. Hafner, C. Mink, H. J. Lindner, *Angew. Chem. Int. Ed. Engl.* **1994**, *33*, 1479.
- [56] Herberhold et al. have recently reported the synthesis and structure of  $[\text{Ru}(\eta\text{-C}_2\text{H}_4\text{CMe}_2)_2]$  (average tilt angle ( $\alpha$ )  $\approx 31^\circ$ ), see M. Herberhold, T. Bärtl, *Z. Naturforsch.* **1995**, *50b*, 1692.
- [57] Y. Ni, R. Rulkens, J. K. Pudelski, I. Manners, *Makromol. Chem. Rapid Commun.* **1995**, *16*, 637.
- [58] N. P. Reddy, H. Yamashita, M. Tanaka, *J. Chem. Soc. Chem. Commun.* **1995**, 2263.
- [59] C. U. Pittman, J. C. Lai, D. P. Vanderpool, M. Good, R. Prado, *Macromolecules* **1970**, *6*, 746.
- [60] W. H. Morrison, S. Krogsrud, D. N. Hendrickson, *Inorg. Chem.* **1973**, *12*, 1998.
- [61] O. W. Webster, W. Mahler, R. E. Benson, *J. Am. Chem. Soc.* **1962**, *84*, 3678.
- [62] J. Stanley, D. Smith, B. Latimer, J. P. Devlin, *J. Phys. Chem.* **1966**, *70*, 2011.
- [63] M. F. Rettig, R. M. Wing, *Inorg. Chem.* **1969**, *8*, 2685.
- [64] D. M. Duggan, D. N. Hendrickson, *Inorg. Chem.* **1975**, *14*, 955.
- [65] R. Prins, A. R. Korswagen, *J. Organomet. Chem.* **1970**, *25*, C74.
- [66] J. S. Miller, D. T. Glatzhofer, D. M. O'Hare, W. M. Reiff, A. Chakraborty, A. J. Epstein, *Inorg. Chem.* **1989**, *28*, 2930.
- [67] J. S. Miller, D. M. O'Hare, A. Chakraborty, A. J. Epstein, *J. Am. Chem. Soc.* **1989**, *111*, 7853.
- [68] J. S. Miller, J. H. Zhang, W. M. Reiff, D. A. Dixon, L. D. Preston, A. H. Reis, E. Gebert, M. Extine, J. Troup, A. J. Epstein, M. D. Ward, *J. Phys. Chem.* **1987**, *91*, 4344.
- [69] M. D. Ward, D. C. Johnson, *Inorg. Chem.* **1987**, *26*, 4213.
- [70] M. D. Ward, P. J. Fagan, J. C. Calabrese, D. C. Johnson, *J. Am. Chem. Soc.* **1989**, *111*, 1719.
- [71] Data were collected on an Enraf Nonius CAD-4 diffractometer with graphite-monochromated  $\text{MoK}_\alpha$  radiation ( $\lambda = 0.71073 \text{ \AA}$ ). The intensities of three standard reflections measured every 120 minutes showed no decay. The data were corrected for Lorentz and polarization effects and an empirical absorption correction was applied (G. M. Sheldrick, SHELX-90, Program for Absorption Correction, University of Göttingen (Germany), **1990**). Minimum and maximum absorption corrections were 0.2547 and 0.8874. The structures were solved and refined with the SHELXTL\PC package (G. M. Sheldrick, SHELXTL\PC, Siemens Analytical X-ray Instruments Inc., Madison, Wisconsin (USA), **1994**). Refinement was by full-matrix least-squares on  $F^2$  using all data (negative intensities included). The weighting scheme was  $w = 1/[\sigma^2(F_o^2) + (0.0549P)^2 + 7.08P]$  where  $P = (F_o^2 + 2F_c^2)/3$ . Hydrogen atoms included in calculated positions. The  $-\text{CH}_2-\text{CH}_2-$  bridge is disordered over two sites with relative occupancies C11A/C12A:C11B/C12B of 60:40.